

## ENHANCING SEISMIC CAPACITY BY APPLYING SILICONE ON WALL-SUPPORTED OFC IN BUILDINGS

George C. Yao<sup>1</sup>, Wen-Chun Huang<sup>2</sup>, and Lei-Man Mak<sup>3</sup>

<sup>1</sup> Professor, Dept. of Architecture, Cheng Kung University, Tainan, Chinese Taiwan

<sup>2</sup> Ph.D. candidate, Dept. of Architecture, Cheng Kung University, Tainan, Chinese Taiwan

<sup>3</sup> Master, Dept. of Architecture, Cheng Kung University, Tainan, Chinese Taiwan

Email: [gcyao@mail.ncku.edu.tw](mailto:gcyao@mail.ncku.edu.tw), [n7689123@nckualumni.org.tw](mailto:n7689123@nckualumni.org.tw), [arc918@yahoo.com.tw](mailto:arc918@yahoo.com.tw)

### ABSTRACT :

This paper studies a non-intrusive fixture method to enhance the seismic capacity of operational and functional components (OFC) supported on walls to avoid damaging the wall and the OFC when installing. The force-displacement relationship of a simulated cabinet adhered by silicone to a wall was determined experimentally and a simplified equation to estimate for the strength of silicone adhesion by simulating the welding design concept is derived. Testing results showed that the strength of applying silicone is dominated by the out-of-plane loading. The lateral strength of 3 N/cm, about 63% weaker than the in-plane one, is proportional to the total installation lengths of the silicone runs. In addition, by performing three-axes shaking table experiment verified that a cabinet carrying 100kg contents can be prevented from toppling with a safety factor of 1.5 if adhered with leg size 2cm, length 120cm silicone runs on two sides of the cabinet.

**KEYWORDS:** OFC, Silicone, Seismic capacity, Silicone Adhesion, Adhering strength

### 1. INTRODUCTION

After experiencing great losses caused by the major damaging earthquakes in many countries, the aseismic design of buildings in areas of severe seismic hazards has been significantly improved in recent years. The structural components, such as columns, beams, and walls, of the buildings definitely protect people from injury, or death, in severe earthquakes. However, the economic losses due to seismic events can not be significantly reduced unless both structural and non-structural components of a building are well designed. Non-structural components, providing the functionalities of a building, are also known as the operational and functional components (OFC). Three groups, architectural components, building service components, and building contents, are included in the OFCs [Foo et al., 2007]. This paper focuses on the seismic capacity of the building components, such as the cabinet, shelves, and storage cases that are situated next to the walls.

Traditionally, the metal angles for a rigid connection were suggested to secure a cabinet on neighboring walls [Fierro et al, 1994], as shown in Fig. 1. This approach itself damages both the cabinet and the supporting walls and may be particularly unacceptable in situations such as expensive or sensitive equipment that demands manufacturer warranty.

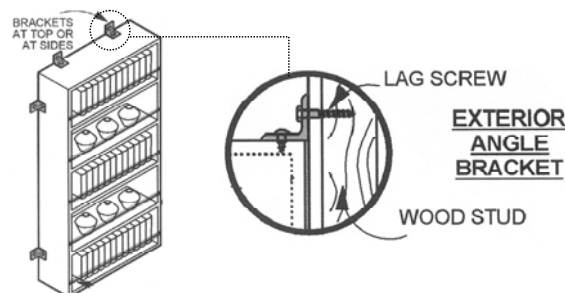


Figure 1. Metal angles for a rigid connection of a cabinet on neighboring walls [Fierro et al, 1994]

A new fixture technique to avoid the above said problems by adhering cabinets to a neighboring wall by silicone

was discussed in the authors' previous research [Yao and Mak, 2007]. For light-weight OFC situated next to a wall, silicone connection is the convenient glue for seismic protection. It is inexpensive and causes no surface damage to the wall and OFC. The strength of silicone adhesion is demonstrated in the paper with experimental results and a simple equation is derived for application. Static push tests indicated that the ultimate strength of the silicone adhering can provide cabinets lateral resistance and exhibit some ductility after the initial yielding. However, in the study, [Yao and Mak, 2007] only the static strength of silicone adhering in the in-plane direction of the supporting wall, as shown in Fig. 2(a), was discussed. This research studies the silicone adhering strength in the out-of-plane direction of the supporting wall, as shown in Fig. 2(b), and performs the dynamic shaking table experiments. Experimental study is performed to investigate the behavior of the silicone runs as well as to calibrate the theoretically calculated strength.

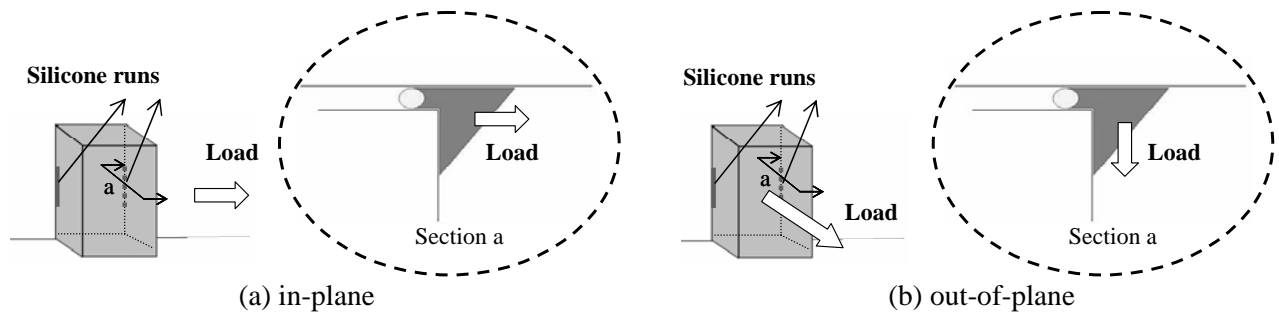


Figure 2. Silicone adhesion resists the load in different directions of the supporting wall

## 2. THE PROPERTIES OF SILICONE

Silicone has excellent property in waterproofing, anti-oxidizing, weatherproofing, and its operational temperature could be widely between  $-50^{\circ}\text{C}$  to  $250^{\circ}\text{C}$ . There are some significantly useful properties of silicone for applied as material of interiorly seismic resistance during earthquakes as following [Dow Corning, 2005]:

1. Most types of silicone have effective tensile strengths  $F_u$  up to 0.55MPa after a week from application.
2. It produces no unpleasant scent during and after application of silicone.
3. Silicone has good bonding strength for many types of building materials such as wood, Paint Coating Steel Sheets (PCSC), concrete surface, glass, etc.

## 3. THE THEORETICAL CALCULATION FOR STRENGTH OF SILICONE ADHESION

This research utilizes the equations for fillet welds to estimate the strength of silicone adhesion. Fillet weld strength is generally calculated by the multiplication of allowable shear stress  $F_a$  and effective throat area  $A_e$  [Spiegel and Limbrunner, 1997].  $A_e$  is calculated by:

$$A_e = t \times L \quad (3.1)$$

where  $t$  is the effective length of the weld throat, and  $L$  is the total length of the fillet weld.  $t$  can be determined from  $a$ , the leg size of weld section assuming equal on both legs, as shown in Fig. 3. However,  $t$  is different based on the direction of the force with respect to the run direction of the welds. If it is a parallel loading, shown in Fig. 3(a),  $t$  will be different from that of the perpendicular loading shown in Fig. 3(b). The equation for calculating  $t$  is shown as:

$$t = \begin{cases} 0.707 \cdot a, & \text{for parallel loading} \\ 0.766 \cdot a, & \text{for perpendicular loading} \end{cases} \quad (3.2)$$

Multiplying the allowable shear stress  $F_a$  and effective throat area  $A_e$ , and substituting Eq. 3.2 to Eq. 3.1, the strength of welded connection  $P_w$  can be calculated by:

$$P_w = \begin{cases} F_a \times A_e = F_a \times 0.707 \cdot a \times L, & \text{for parallel loading} \\ F_a \times A_e = F_a \times 0.766 \cdot a \times L, & \text{for perpendicular loading} \end{cases} \quad (3.3)$$

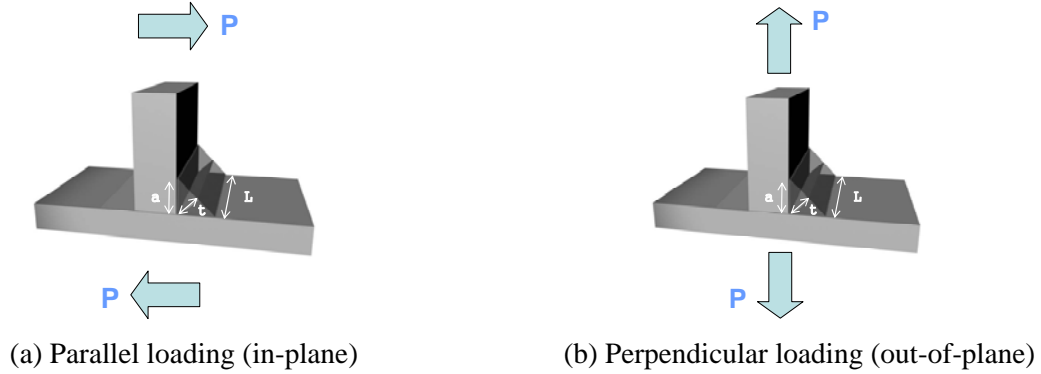


Figure 3. Terminology in welding

Eq. 3.3 reveals that the weld strength  $P_w$  of the perpendicular loading is larger than that of the parallel loading. The in-plane loading direction and the out-of-plane loading direction correspond to parallel loading direction and the perpendicular loading direction, respectively. However, experimental results show that the silicone adhesion exhibits higher strength of the in-plane loading than that of the out-of-plane loading. This is a significant difference between the strength of weld and of silicone adhesion. In order to correct the estimation for the strength of the silicone adhesion, we propose only using  $t = 0.707a$  to account for all silicone runs irrespective of the loading direction, and the allowable shear strength  $F_a$  should be reduced by a reduction factor  $\rho$  as shown in Eq. 3.4:

$$F_a = \rho \times F_u \quad (3.4)$$

where  $F_u$  is the tensile strength of the adhesion material, and  $\rho$  is usually set 0.3 in the welding design. In this study, the value of  $\rho$  for different types of silicone, interfaces and loading directions are determined by the experimental results. Therefore, the strength of the DC-795 silicone runs  $P_s$  can be estimated by:

$$P_s = \begin{cases} \rho_i \times F_u \times 0.707 \cdot a \times L, & \text{for in-plane loading} \\ \rho_o \times F_u \times 0.707 \cdot a \times L, & \text{for out-of-plane loading} \end{cases} \quad (3.5)$$

In this paper, the DC-795 [Dow Corning, 2005] from the Dow Corning is chosen for study. In comparison, a generic brand from a local hardware store, B&Q, is also tested. Dow Corning recommends DC-795 as the structural sealant for curtain wall application to secure glass on the curtain wall frame. The tensile strength  $F_u$  of DC-795 is 0.55MPa from the Dow Corning. The tensile strength  $F_u$  of the B&Q silicone is not available from the B&Q, therefore  $F_u = 0.55\text{MPa}$  is also assumed for the B&Q silicone. Strength differences between the DC-795 and the B&Q silicone would be presented by various  $\rho$  which are determined by the experiments.

#### 4. THE EXPERIMENTAL STUDY

Three series of experiments, in-plane static push tests, out-of-plane static push tests, and three-axes dynamic shaking table tests, are performed in this study. Two types of silicone, DC-795 and a generic brand B&Q, were tested in full-scale to identify the strength of silicone runs.

##### 4.1. The in-plane static push test

The in-plane test setup illustration and the pictures are shown in Figure 4. Two vertical planks with finished concrete surface were simulated a concrete wall in a building. These two planks were fixed at top and bottom to a rigid steel frame. Only the left-hand side column is shown, the right-hand side column on the rigid steel frame is not shown in Fig. 4 for clarity of the figure. A concrete block was used to simulate cabinets or any OFCs alike. Two edges of the block were adhered to the planks at the back by silicone to simulate actual silicone runs on cabinets against a wall. Two runs of silicone each with a length of 80cm were applied to join the block and the planks.

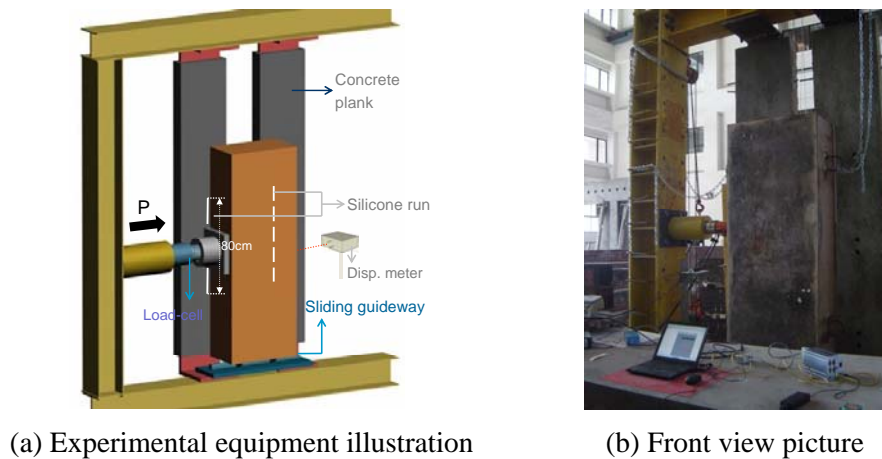


Figure 4. The in-plane loading test setup

Two different types, wood finish and PCSC, of surface finish to simulate OFC exterior were attached on the edges of the concrete block where silicone was applied. Therefore the adhesive strength between different interfaces of wood vs. concrete and PCSC vs. concrete can be compared. Two leg sizes,  $a = 1\text{ cm}$  and  $a = 2\text{ cm}$ , of the silicone runs were chosen for each surface finishes in order to verify the strength of different silicone sizes. Static tests were performed by providing an incremental horizontal force to push the concrete block in Fig. 4 until the silicone runs can no longer provide any strength. In order to reduce the friction forces at the bottom of the concrete block, a linear sliding guideway was placed under the concrete block. The frictional forces provided by the linear guideway were measured and adjusted in the final data.

Testing results are shown in Fig. 5. It reveals that increasing the leg size by 100% from 1 cm to 2 cm, the ultimate strength increased to about 150% in most of the tests. The B&Q silicone performs just as well as the DC-795 even with a slightly higher strength, and this result verifies the preceding assumption of  $F_u = 0.55\text{ MPa}$  for the B&Q silicone is not over estimated and could be acceptable. However, although the strengths of B&Q and DC-795 are similar, but the deformation capacity at the beginning of sharp strength degradation after ultimate stress observed, DC-795 tends to have a larger deformation capacity than that of the B&Q silicone.

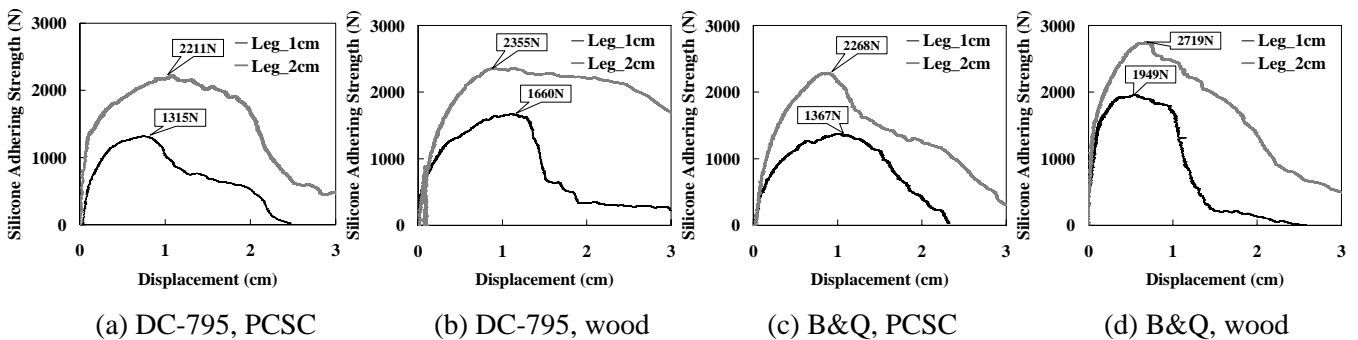


Figure 5. The force-displacement curves of in-plane loading test

The failure patterns between different interfaces are shown in Fig. 6. Some of the tests failed with complete detachment from the concrete finish, as shown in Fig. 6(a) and Fig. 6(d); some with silicone remains still attached to the concrete finish after testing, as shown in Fig. 6(b). The severest damage occurred in the case of B&Q silicone applied on PCSC vs. concrete interface. The silicone was fractured, some remained on concrete wall, and some remained on PCSC finish of the specimen, as shown in Fig. 6(c). This observation shows again that the DC-795 silicone tends to have a better deformation capacity than that of the B&Q silicone.

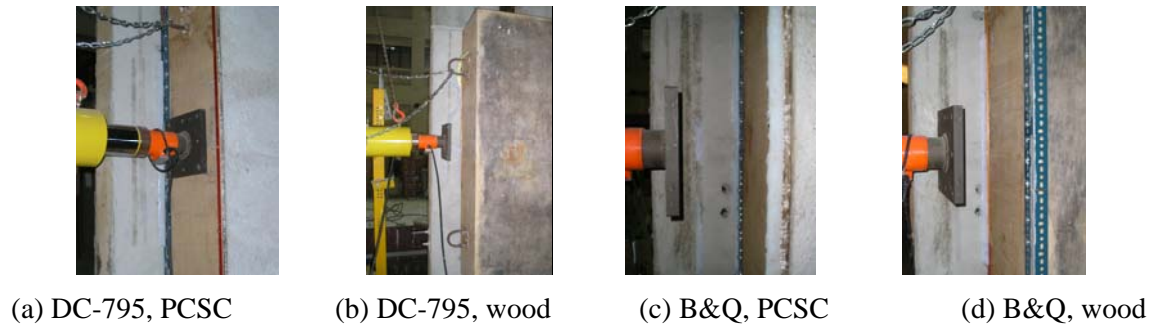


Figure 6. The failure patterns of in-plane loading tests

#### 4.2. The out-of-plane static push test

In the out-of-plane loading test, the experimental setup was altered and the specimen was perpendicularly turned from the in-plane loading test, as shown in Fig. 7(a). A concrete finished steel plate with an opening was fixed between two planks so that the specimen could be adhered to the steel plate with silicone. The actuator can exert the out-of-plane loading to the specimen, as shown in Fig. 7(b) and Fig. 7(c). Other experimental variables, such as leg sizes, lengths of silicone runs, and the interface conditions are all the same as those in the in-plane loading test.

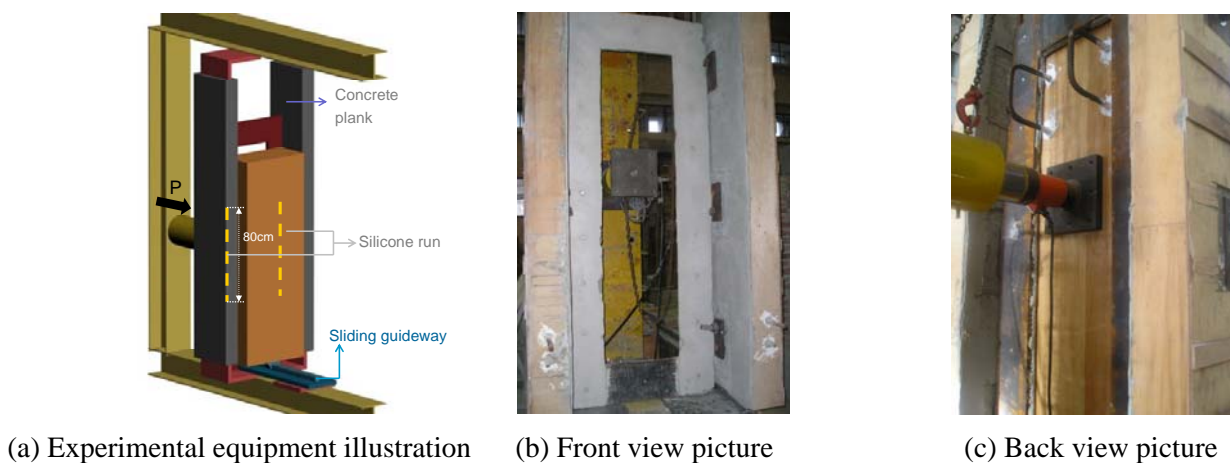


Figure 7. The out-of-plane loading test setup

Testing results are shown in Fig. 8. Similar to the results of the in-plane test, the B&Q silicone has a slightly larger strength, about 10%, than the DC-795 silicone, but the DC-795 silicone has better deformation capacity than the B&Q silicone. Doubling the leg sizes from 1cm to 2cm, the strength could only rise about 50%. It is found the out-of-plane loading strength of silicone adhesion, reducing to about 37% of the in-plane ones, is much weaker and therefore dominates the seismic capacity of silicone runs. This behavior is different from the welded connection, which has larger strength in perpendicular direction than in the parallel direction. Considering this difference, both of the in-plane reduction factor  $\rho_i$  and the out-of-plane reduction factor  $\rho_o$  are determined by the experimental data and therefore the strengths of the silicone adhesion could be adequately estimated by Eq. 3.5 in both directions.

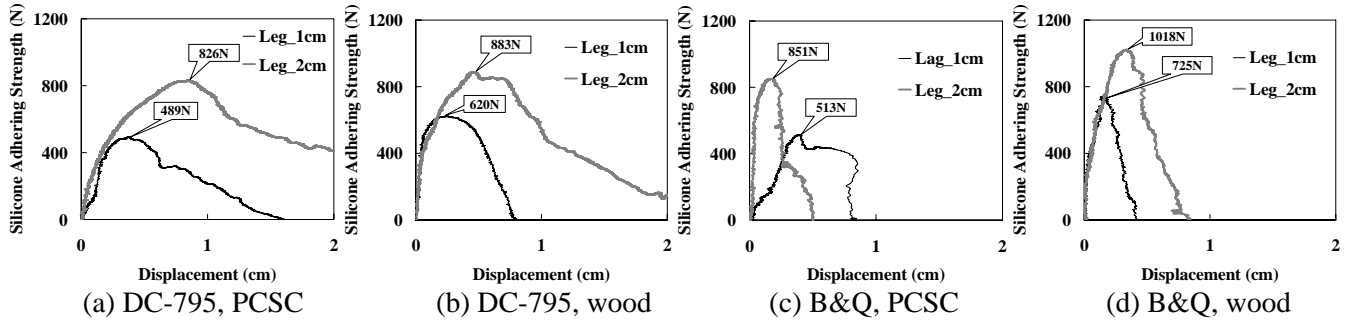


Figure 8. The force-displacement curves of out-of-plane loading tests

The failure modes of out-of-plane loading tests are shown in Fig. 9. Regardless of using DC-795 or the B&Q silicone, both interfaces of PCSC vs. concrete and wood vs. concrete failed with silicone complete detachment from the concrete finish.

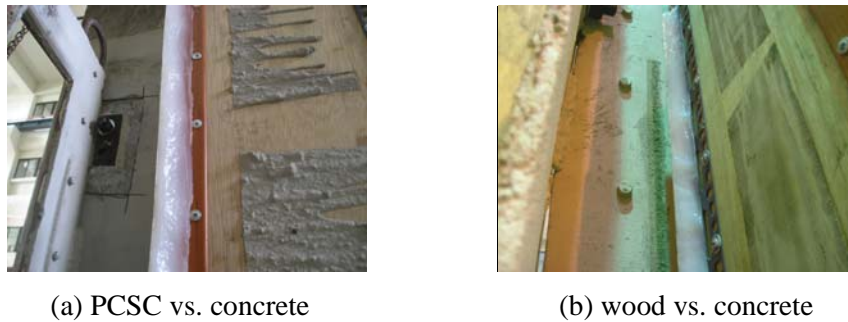


Figure 9. The failure modes of silicone runs in out-of-plane loading tests

#### 4.3. Determination of the reduction factor $\rho$ from experimental data

By rearranging Eq. 3.5, the reduction factor  $\rho$  of silicone adhesion can be calculated by:

$$\rho_i = \frac{P_{si}}{F_u \times 0.707 \cdot a \times L}, \text{ for in-plane loading} \quad (3.6)$$

$$\rho_o = \frac{P_{so}}{F_u \times 0.707 \cdot a \times L}, \text{ for out-plane loading}$$

where  $P_{si}$  and  $P_{so}$  are the in-plane strength and out-of-plane strength of the silicone adhesion, respectively. For example, if DC-795 silicone were applied with leg size 1cm, length of silicone adhesion runs 80cm on two sides (totally 160cm). Since  $P_{si} = 1315\text{N}$  and  $P_{so} = 489\text{N}$  were measured from the experiments, then  $\rho_i$  and  $\rho_o$  could be determined by:

$$\rho_i = \frac{1315\text{N}}{0.55\text{MPa} \times 0.707 \cdot 10\text{mm} \times 160\text{mm}} = 0.21, \text{ for in-plane loading}$$

$$\rho_o = \frac{489\text{N}}{0.55\text{MPa} \times 0.707 \cdot 10\text{mm} \times 160\text{mm}} = 0.08, \text{ for out-plane loading}$$

Other reduction factors for various experimental conditions in this study are shown in Table 4.1. Obviously, the out-of-plane reduction factor  $\rho_o$  is smaller than the in-plane factor  $\rho_i$ . It may be conservatively designing values of  $\rho_i = 0.18$  and  $\rho_o = 0.07$ . The strengths of silicone adhesion are controlled by the out-of-plane loading under multiple-direction earthquake forces. Besides, from Table 4.1, the strengths of silicone provided per unit length could be estimated as from  $8.2\text{ N/cm}$  to  $14.7\text{ N/cm}$  in the in-plane loading direction and from  $3.1\text{ N/cm}$  to  $6.4\text{ N/cm}$  in the out-of-plane loading direction.

Table 4.1. The reduction factor  $\rho$  of various types of silicone and loading directions  
(total silicone run length = 160cm)

| Type of silicone and interface | Leg $a$<br>(cm) | Total $L$<br>(cm) | $F_u$<br>(MPa) | In-plane<br>strength<br>$P_{si}$ (N) | In-plane<br>$\rho_i$ | Out-of-plane<br>strength $P_{so}$<br>(N) | Out-of-plane<br>$\rho_o$ |
|--------------------------------|-----------------|-------------------|----------------|--------------------------------------|----------------------|--|--------------------------|
| DC-795, PCSC vs. concrete      | 1               | 160               | 0.55           | 1315                                 | <b>0.21</b>          | 489                                      | <b>0.08</b>              |
| DC-795, wood vs. concrete      | 1               | 160               | 0.55           | 1660                                 | <b>0.27</b>          | 620                                      | <b>0.10</b>              |
| B&Q, PCSC vs. concrete         | 1               | 160               | 0.55           | 1367                                 | <b>0.22</b>          | 513                                      | <b>0.08</b>              |
| B&Q, wood vs. concrete         | 1               | 160               | 0.55           | 1949                                 | <b>0.31</b>          | 725                                      | <b>0.12</b>              |
| DC-795, PCSC vs. concrete      | 2               | 160               | 0.55           | 2211                                 | <b>0.18</b>          | 826                                      | <b>0.07</b>              |
| DC-795, wood vs. concrete      | 2               | 160               | 0.55           | 2355                                 | <b>0.19</b>          | 883                                      | <b>0.07</b>              |
| B&Q, PCSC vs. concrete         | 2               | 160               | 0.55           | 2268                                 | <b>0.18</b>          | 851                                      | <b>0.07</b>              |
| B&Q, wood vs. concrete         | 2               | 160               | 0.55           | 2719                                 | <b>0.22</b>          | 1018                                     | <b>0.08</b>              |

#### 4.4. Three axes shaking table test

The dynamic shaking table test is performed to verify if the silicone adhesion can resist the loadings under vibrations generated from multiple directions. A model house composed of steel frames was utilized to simulate the place where the OFCs is located in, as shown in Fig. 10. The model house was mounted on a 5.1m  $\times$  5.1m shaking table in the NCREE in Taipei. A cabinet with PCSC finish was used as the specimen, and five steel plates, each weighs 20kg, totally 100kg, were put in the cabinet, as shown in Fig. 11(a). Two B&Q silicone runs with leg size 2cm, and length 120cm were applied on two sides of the cabinet, as shown in Fig. 11(b) and Fig. 11(c). From the reduction factors determined in Table 4.1, the strength of the silicone runs were 4752N and 1848N in the directions of in-plane and out-of-plane, respectively. In the figure, the metal angles were used to fix the cabinet until the silicone was solidified for a week, and the metal angles were removed before start testing.



Figure 10. The modeling house made of steel frames



Figure.11. Installation of the cabinet for testing

The experimental setup was shown in Fig. 12. The input excitations were generated from the response spectra in accordance with AC156 [ICC, 2006], the acceptance criteria of shaking table test for non-structural components suggested by ICC-ES, Inc. According to aseismic code in Taiwan, the maximum horizontal input acceleration is about 1.28g, and that in the vertical direction is about 0.53g, as shown in Fig. 13. The figure shows the achieved peak accelerations of real input excitations, about 2.0g in horizontal, 1.0g in vertical, are higher than those suggested in the code. However, the result is considered as being acceptable and conservative because the 100kg-weighted cabinet and the silicone runs were not damaged after experiencing the multiple direction excitation forces equaling to at least  $2.0g \times 9.81m/sec^2 \times 100kg = 1962N$ . This test result indicates that appropriately applying silicone can at least provide a safety factor of 1.5 ( $\approx 2g/1.28g$ ) in the dynamic environment for silicone strength calculation based on the static tests.

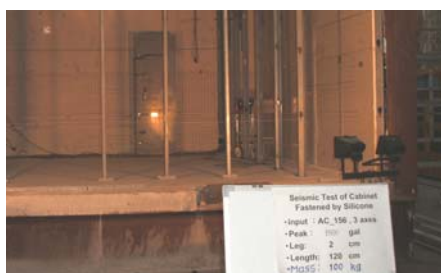


Figure 12. The experimental setup of shaking table test for cabinet adhered by silicone

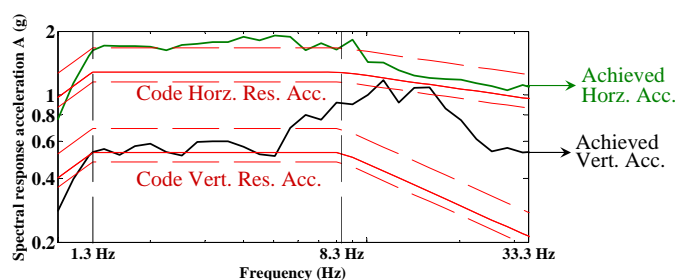


Figure 13. The input acceleration spectra of the shaking table test

## 5. CONCLUSIONS

In this paper, a new connection technique of a non-intrusive approach by applying silicone as the adhesive material for wall-supported OFC is proposed. A simple equation derived from the fillet weld design is proposed for the silicone adhesion since both of them have similar geometric layout. Static push tests were performed to compare the actual ultimate strengths with the calculated values. The dynamic shaking table test was conducted to verify the efficiency of application of silicone adhesion in protecting cabinets or other OFCs alike. Some significant points were investigated as following:

1. Using the fillet weld designing equation can estimate for the strength of silicone adhesion if reduction factor  $\rho$  were determined adequately. For conservative consideration,  $\rho_i = 0.18$  and  $\rho_o = 0.07$  are suggested from experimental results in this study.
2. Testing results reveal that the ultimate strength of the silicone adhesion for raising leg size from 1cm to 2cm only rises 50% of the strength irrespective of surface finish. The out-of-plane loading strength of the silicone run is about 37% of that of the in-plane loading.
3. Two types of silicone used in the tests exhibited similar strength. It is also found that the DC-795 silicone exhibited more ductility after the initial yielding during the tests.
4. The efficiency of application has been verified by dynamic shaking table test with input waves generated in accordance with the response spectra for non-structural components suggested by AC156.

## ACKNOWLEDGEMENT

This research is supported partially by the NSC in Taiwan under a grant project of NSC-95-2625-Z-006-008. The static experiments were conducted in the structural laboratory of Dept. of Architecture, NCKU in Tainan and the shaking table tests were conducted in the NCREC in Taipei.

## REFERENCES

- Dow Corning. (2005). Technical Manual. Dow Corning, USA.
- Foo, S., Ventura C.E. and McClure G. (2007). An Overview of a New Canadian Standard on the Seismic Risk Reduction of Operational and Functional Components of Buildings. *Proceeding of 9<sup>th</sup> Canadian Conference on Earthquake Engineering*, **1361**, Ottawa, Canada.
- Fierro, E.A., Perry, C.L. and Freeman S.A. (1994). Reducing the Risks of Nonstructural Earthquake Damage—A Practical Guide. The Federal Emergency Management Agency (FEMA), under the National Earthquake Technical Assistance Contract, USA.
- ICC Evaluation Service, Inc. (2006). Acceptance Criteria for Seismic Qualification by Shaking-Table Testing of Nonstructural Components and Systems. ICC Evaluation Service, Inc., USA.
- Spiegel, L. and Limbrunner, G.F. (1997). Applied Structural Steel Design. Regents/ Prentice-Hall, USA
- Yao, G.C. and Mak, L.M. (2007). A New Technique for Wall-Supported OFC in Buildings. *Proceeding of 9<sup>th</sup> Canadian Conference on Earthquake Engineering*, **1011**, Ottawa, Canada.